

The cosmic ray elemental composition based on measurement of the N_μ/N_{ch} ratio with KASCADE-Grande

E. CANTONI^{1,7}, W.D. APEL², J.C. ARTEAGA-VELÁZQUEZ³, K. BEKK², M. BERTAINA¹, J. BLÜMER^{2,4}, H. BOZDOG², I.M. BRANCUS⁵, P. BUCHHOLZ⁶, A. CHIAVASSA¹, F. COSSAVELLA^{4,13}, K. DAUMILLER², V. DE SOUZA⁸, F. DI PIERRO³, P. DOLL², R. ENGEL², J. ENGLER², M. FINGER⁴, D. FUHRMANN⁹, P.L. GHIA⁷, H.J. GILS², R. GLASSTETTER⁹, C. GRUPEN⁶, A. HAUNGS², D. HECK², J.R. HÖRANDEL¹⁰, D. HUBER⁴, T. HUEGE², P.G. ISAR^{2,14}, K.-H. KAMPERT⁹, D. KANG⁴, H.O. KLAGES², K. LINK⁴, P. ŁUCZAK¹¹, M. LUDWIG⁴, H.J. MATHES², H.J. MAYER², M. MELISSAS⁴, J. MILKE², B. MITRICA⁵, C. MORELLO⁷, G. NAVARRA^{1,15}, J. OEHLISCHLÄGER², S. OSTAPCHENKO^{2,16}, S. OVER⁶, N. PALMIERI⁴, M. PETCU⁵, T. PIEROG², H. REBEL², M. ROTH², H. SCHIELER², F.G. SCHRÖDER², O. SIMA¹², G. TOMA⁵, G.C. TRINCHERO⁷, H. ULRICH², A. WEINDL², J. WOCHLE², M. WOMMER², J. ZABIEROWSKI¹¹

¹ *Dipartimento di Fisica Generale dell' Università Torino, Italy*

² *Institut für Kernphysik, KIT - Karlsruher Institut für Technologie, Germany*

³ *Universidad Michoacana, Instituto de Física y Matemáticas, Morelia, Mexico*

⁴ *Institut für Experimentelle Kernphysik, KIT - Karlsruher Institut für Technologie, Germany*

⁵ *National Institute of Physics and Nuclear Engineering, Bucharest, Romania*

⁶ *Fachbereich Physik, Universität Siegen, Germany*

⁷ *Istituto di Fisica dello Spazio Interplanetario, INAF Torino, Italy*

⁸ *Universidade São Paulo, Instituto de Física de São Carlos, Brasil*

⁹ *Fachbereich Physik, Universität Wuppertal, Germany*

¹⁰ *Dept. of Astrophysics, Radboud University Nijmegen, The Netherlands*

¹¹ *Soltan Institute for Nuclear Studies, Lodz, Poland*

¹² *Department of Physics, University of Bucharest, Bucharest, Romania*

¹³ *now at: Max-Planck-Institut Physik, München, Germany;* ¹⁴ *now at: Institute Space Sciences, Bucharest, Romania;* ¹⁵ *deceased;* ¹⁶ *now at: Univ Trondheim, Norway*
cantoni@to.infn.it, achivass@to.infn.it

DOI: 10.7529/ICRC2011/V01/0504

Abstract: The KASCADE-Grande experiment, located at Karlsruhe Institute of Technology, is a multi-component Extensive Air Shower (EAS) detector studying primary cosmic rays in the $10^{16} - 10^{18}$ eV energy range. In this contribution a measurement of the cosmic ray chemical composition, based on the comparison of the experimental distributions of the ratio between the EAS muon size and the total charged size (N_μ/N_{ch}) with those expected from a complete EAS simulation based on the QGSJet II-03 interaction model, is presented. It has already been shown that, in the frame of this interaction model, the detector performances allow to separate three different mass groups: light, intermediate and heavy. With the employed technique, the relative abundances of the three mass groups are derived and their evolution as a function of the charged particle size is observed. The differential spectra of the three mass groups are then inferred and discussed

Keywords: Composition, KASCADE-Grande

1 Introduction

The energy range from 10^{16} to 10^{18} eV is very important to deeply investigate the details of the knee of the primary energy spectrum. In the last ten years different experiments (e.g. KASCADE [1] and EAS-TOP [2]) have shown that this feature can be attributed to the light component of the primaries (i.e. H or He). A definitive confirmation of the astrophysical origin of the knee can only be obtained by

the detection of the foreseen change of slope of the heavy component at a primary energy $\sim 10^{17}$ eV.

In this contribution we present a study of the primary cosmic ray chemical composition in the $10^{16} - 10^{18}$ eV energy range performed comparing the KASCADE-Grande experiment [3] data with the results of a full Extensive Air Shower simulation based on the CORSIKA [4] code and on the QGSJet II-03 [5] interaction model.

The KASCADE-Grande experiment is located at the Campus North of the Karlsruhe Institute of Technology, 110

m a.s.l. It consists of an array of 37 plastic scintillator modules 10 m^2 each (Grande) spread over an area of $700 \times 700 \text{ m}^2$, working jointly with the co-located and formerly present KASCADE experiment [6], consisting of 252 electron and muon scintillation detectors placed over a $200 \times 200 \text{ m}^2$ area. All events triggering a sevenfold coincidence of Grande array detectors, arranged on an hexagonal grid (mean side length of 130 m), are reconstructed. The charged particle size N_{ch} is determined by the Grande array and the muon number N_μ by the KASCADE array. Both (N_{ch}) and (N_μ) are measured with an accuracy $\leq 15\%$; a detailed description of the reconstruction procedure can be found in [3].

2 The Chi Square Method

The present analysis is performed, to minimize effects of a possible incorrect description (in the simulation) of the EAS evolution in atmosphere, on vertical events ($0^\circ \leq \theta \leq 24^\circ$). Data are divided in twelve N_{ch} intervals (from $\text{Log } N_{ch}=6.0$ to $\text{Log } N_{ch}=8.0$) and the N_μ/N_{ch} experimental distributions are fitted with a linear combination of those obtained by a complete simulation of events generated with a power law distribution in the $10^{15} - 10^{18} \text{ eV}$ energy range for five different primaries (H, He, C, Si, Fe). We have already shown that the KASCADE-Grande experiment performances allow us to separate, with such algorithm, events into three samples originated by different mass groups [7]. The combination giving the best fits (examples for two of the twelve N_{ch} intervals are shown in figures 1 and 2) is the one composed by the following mass groups: light, 100% hydrogen; intermediate, 50% helium and 50% carbon; heavy, 50% silicon and 50% iron. The linear combination of the simulated mass groups is expressed as follows:

$$F_{sim}(i) = \sum_j \alpha_j f_{sim,j}(i) \quad (1)$$

where $F_{sim}(i)$ is the total theoretical fraction of simulated events falling in the histogram channel i , $f_{sim,j}(i)$ is the fraction for the single component j ($j = 1,2,3$), $\sum_j(i)$ is the sum over the different components and α_j is the fit parameter representing the relative abundance of the component j . The fit parameters fulfill the conditions

$$0. \leq \alpha_j \leq 1. \quad (2)$$

and

$$\sum_j \alpha_j = 1. \quad (3)$$

The fit is performed minimizing the following Chi Square function:

$$\chi^2 = \sum_i \frac{(F_{exp}(i) - F_{sim}(i))^2}{\sigma(i)^2} \quad (4)$$

where $F_{exp}(i)$ is the fraction of experimental events falling in the histogram channel i and $\sigma(i)$ is the error on the theoretical

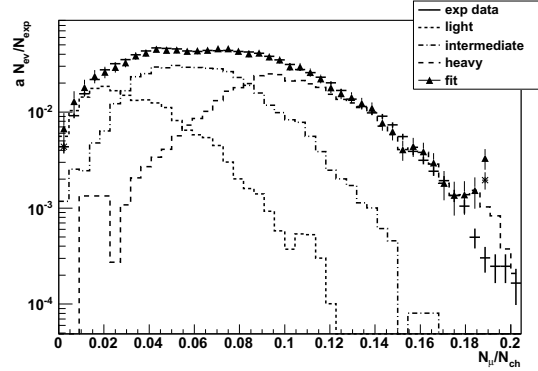


Figure 1: The experimental N_μ/N_{ch} distribution (solid line) measured in the $6.24 \leq \text{Log}(N_{ch}) < 6.36$ interval for vertical events ($0^\circ \leq \theta \leq 24^\circ$) fitted by a combination of Hydrogen (thin dashed line), Helium + Carbon in a 50% mixture (dot dashed line) and Silicon + Iron in a 50% mixture (thick dashed line). The triangles show the fit result. The experimental plot is normalized to 1 and every simulated component is normalized to its relative abundance. The tails of the experimental distribution are treated summing the events (the corresponding value is shown by a star) in a single bin, in order to have at least 5 events in each of them. In the shown example, the results for the abundances and the fit are: $\alpha_{light} = 0.14 \pm 0.02$; $\alpha_{intermediate} = 0.59 \pm 0.02$; $\alpha_{heavy} = 0.27 \pm 0.01$. The chi square and the cumulative function values are: $\chi^2_0/\nu = 56.52/46 = 1.23$, $P(\chi^2 > \chi^2_0) = 0.14$

expression (1). A fit is validated and the relative abundances of the mass groups are accepted if the cumulative function, $P(\chi^2 > \chi^2_0)$, is included in the $0.05 < P < 0.95$ interval.

The choice of sampling events in bins of the charged particle size is made in order to have a selection depending only on the performances of the experiment and not being influenced by an EAS simulation (as could be in the case of reconstructed energy bins).

The behavior of the relative abundances versus the charged particle size is shown in figure 3. The light and intermediate components show a trend with bigger fluctuations with respect to the heavy mass group. The relative abundance of the light mass group is almost independent on the charged particle shower size, while the heavy one shows a sudden change at $\log N_{ch} \sim 6.8$. The intermediate mass group seems to be more abundant near (in N_{ch} bins) the threshold, decreasing for higher N_{ch} and becoming nearly similar to those of light elements.

3 Spectra of the single mass groups

From the number of events measured in each $\Delta \log(N_{ch})$ interval ($N_{exp}(k)$, $k = 1, 12$) and having determined the

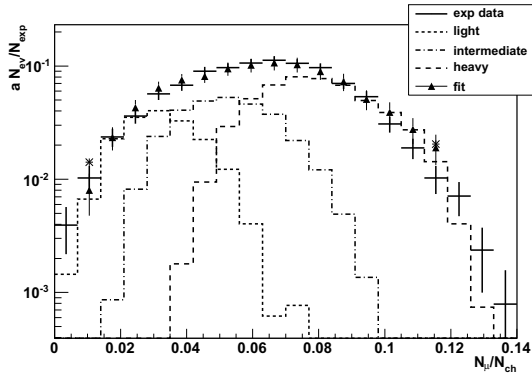


Figure 2: The experimental N_μ/N_{ch} distribution (solid line) measured in the $7.15 \leq \text{Log}(N_{ch}) < 7.24$ interval for vertical events ($0^\circ \leq \theta \leq 24^\circ$) fitted by a combination of light (thin dashed line), intermediate (dot dashed line) and heavy (thick dashed line). The triangles show the fit results. In the shown example, the results for the abundances and the fit are: $\alpha_{light} = 0.16 \pm 0.02$; $\alpha_{intermediate} = 0.30 \pm 0.04$; $\alpha_{heavy} = 0.52 \pm 0.03$. The chi square and the cumulative function values are: $\chi_0^2/\nu = 9.66/14 = 0.69$, $P(\chi^2 > \chi_0^2) = 0.79$

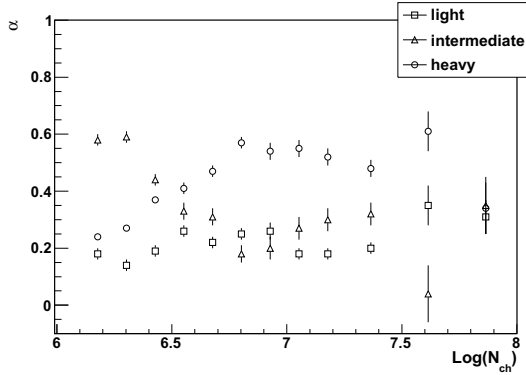


Figure 3: Relative abundances of the three mass groups versus the charged particle size N_{ch} measured for vertical events.

relative abundance of each mass group (j) we can calculate the number of events that are originated by primaries belonging to the j^{th} mass group ($N_j(k) = \alpha_j \cdot N_{exp}(k)$). The three mass group fluxes in each charged particle size bin are then derived:

$$\Phi_j(k) = N_j(k)/(A\Omega\Delta t)(m^{-2}sr^{-1}s^{-1}) \quad (5)$$

where $A = 1.52 \times 10^4 m^2$, $\Omega = 0.52 sr$ and $\Delta t = 1.1 \times 10^8 s$.

From a full EAS (based on the QGSJet II-03 interaction model) and detector simulation we derive, for each mass group, a power law relation ($E_0 = 10^b \cdot N_{ch}^a$) between the charged particle size and the primary energy (the values of the a and b parameters are reported in table 1). With these

	light	intermediate	heavy
a	0.99 ± 0.01	0.93 ± 0.004	0.91 ± 0.01
b	0.75 ± 0.06	1.30 ± 0.02	1.61 ± 0.03

Table 1: a , b parameters of the power law correlating, for each mass group, the charged particle size N_{ch} and the primary energy E_0

relations we convert the N_{ch} intervals into the corresponding energy bins (that are thus not the same for the three mass groups) and from the measured fluxes we derive the differential flux at the central energy of each interval.

To verify if, through the described algorithm, we are able to reproduce the spectra of the single mass groups we have performed the same analysis on test spectra: half of the simulated data set is used as fake experimental data while the other half is used as reference for the fitting procedure. With the goal of identifying possible spectral distortions artificially introduced by the analysis we have chosen the test spectra with a slope $\gamma = -3$ and without breaks for all elements. The results are shown in figure 4: the heavy mass group shows good agreement between test and reconstructed spectra in the whole energy range. The light and intermediate mass groups are in good agreement for energies greater than 4×10^{16} eV while near the threshold the reconstructed spectra are lower than the test ones. This result is not unexpected as shower and experimental fluctuations (that are bigger for low masses and originate an event migration from bin to bin) are not yet corrected for in the conversion from N_{ch} to energy. This procedure is under development, its results will be shown soon. It is worthwhile to point out that the uncorrected reconstructed test spectra show, for all mass groups, no artificial breaks.

Another hint of the correct behavior of the described analysis algorithm can be derived from figure 5 showing the relative abundances reconstructed for the previously described test spectra. These abundances show no dependence on N_{ch} in the whole range, even if fluctuations (mainly of the light and intermediate mass groups) around the expected value can be seen.

4 Conclusions

The performances of the algorithm aiming at the measurement of the evolution of the primary chemical composition of cosmic rays are described. We have shown how, with the KASCADE-Grande experiment performances, we are able to separate three mass groups and that all of them are needed to reconstruct the measured N_μ/N_{ch} distributions. The measured chemical composition gets heavier as the shower size N_{ch} increases as can be inferred from the evolution of the relative abundances of the three mass groups with N_{ch} .

The measured spectra of the three mass groups are shown in figure 6 as obtained in the frame of the QGSJet II-03

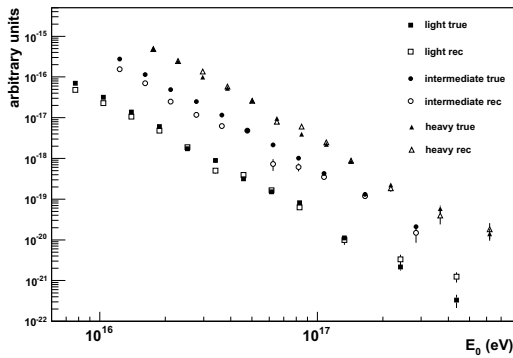


Figure 4: Comparison between test and reconstructed spectra for the three mass groups. In the fake spectrum all mass groups have equal abundance, in the plot the fluxes of light and heavy mass groups are multiplied by arbitrary factors for clarity.

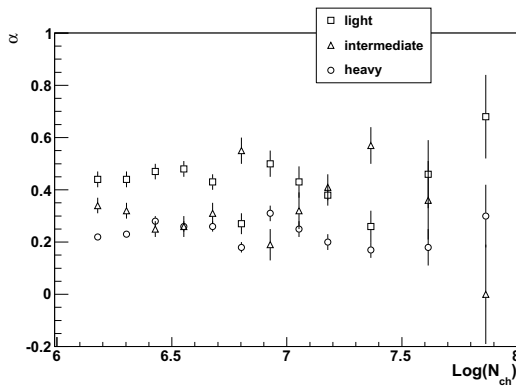


Figure 5: Reconstructed relative abundances of the three mass groups versus the charged particle size N_{ch} obtained analyzing test spectra with constant and equal slope for all elements.

interaction model. The spectrum of the heavy mass group shows a distinct change of slope and cannot be described by a single power law. This reconstructed spectrum is fitted with a function [8] describing a spectral shape with two different slopes interconnected by a smooth knee at energy E_k . The results, shown by the solid line in figure 6, are: $\gamma_1 = 2.67 \pm 0.02$, $\gamma_2 = 3.29 \pm 0.02$ and $\log E_k (eV) = 17.79 \pm 0.04$. The statistical significance of the change of slope is $\sim 4\sigma$. At a similar energy a (weaker) steepening is also observed in the all particle spectrum measured by KASCADE-Grande [9].

In contrast both the intermediate and light mass groups spectra are describable by a single power law due to the low event numbers. These spectra are dominated by statistical fluctuations, and no significant conclusion can thus be derived at the moment.

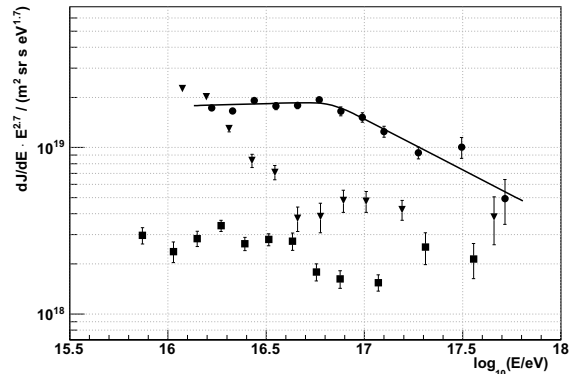


Figure 6: Differential energy spectra of the three mass groups: heavy (Si+Fe, dots), intermediate (He+C, triangles) and light (H, squares) elements.

All shown spectra do not yet take into account effects of event-to-event shower fluctuations at the energy assignment: a procedure to unfold them is under development.

It is important to emphasize that the present results, and in particular the relative abundances of the mass groups, heavily depend on the choice of QGSJet II-03 as interaction model. The entire analysis will be, in near future, repeated on basis of a complete EAS simulation based on a different interaction models, i.e. EPOS [10].

Acknowledgement: KASCADE-Grande is supported by the BMBF of Germany, the MIUR and INAF of Italy, the Polish Ministry of Science and Higher Education and the Romanian Authority for Scientific Research.

References

- [1] W.-D. Apel *et al.* (KASCADE Collaboration), *Astrop. Phys.* **24** (2005) 1.
- [2] M. Aglietta *et al.* (EAS-TOP Collaboration), *Astrop. Phys.* **21** (2004) 583.
- [3] W.-D. Apel *et al.* (KASCADE-Grande Collaboration), *NIM A* **620** (2010) 202.
- [4] D. Heck *et al.*, Report FZKA 6019, Forschungszentrum Karlsruhe (1998).
- [5] S.S. Ostapchenko, *Nucl. Phys. B (Proc. Suppl.)* **151** (2006) 143&147; S. Ostapchenko, *Phys. Rev. D* **74** (2006) 014026.
- [6] T. Antoni *et al.* (KASCADE Collaboration), *NIM A* **513** (2003) 429.
- [7] E. Cantoni *et al.* (KASCADE-Grande Collaboration), *Proc. 31st ICRC, Lodz (Poland) 2009, #0524*
- [8] W.-D. Apel *et al.* (KASCADE Collaboration), *Astrop. Phys.* **16** (2002) 245.
- [9] M. Bertaina *et al.* (KASCADE-Grande Collaboration), *Proc. 31st ICRC, Lodz (Poland) 2009, #0323*
- [10] K. Werner, F.M. Liu, T. Pierog, *Phys. Rev. C* **74** (2006) 044902.